Topology optimisation for large-scale wire-arc directed energy deposition considering environmental impact and cost
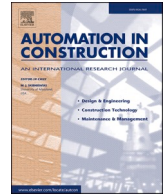
Baqershahi, Mohammad Hassan; Ayas, Can; Ghafoori, Elyas

Important note
To cite this publication, please use the final published version (if applicable).
Please check the document version above.

Topology optimisation for large-scale wire-arc directed energy deposition considering environmental impact and cost

Mohammad Hassan Baqershahi [a],[*], Can Ayas [b], Elyas Ghafoori [a]

[a] *Institute for Steel Construction, Faculty of Civil Engineering and Geodetic Science, Leibniz University Hannover, 30167 Hannover, Germany*
[b] *Department of Precision and Microsystems Engineering, Faculty of Mechanical, Maritime and Materials Engineering, Delft University of Technology, 2628CD Delft, the Netherlands*

ABSTRACT

Advancements in wire-arc directed energy deposition (DED) have created new opportunities for manufacturing efficient large-scale structures. While wire-arc DED is often viewed as more sustainable and economical due to the potential of producing lighter structures, its higher environmental impact and cost per unit of weight necessitate further considerations during the design phase. This paper explores how sustainability and cost can be integrated into conceptual design through topology optimisation. The approach is demonstrated through a case study, including a parametric study on specific environmental impact and the cost of wire-arc DED versus CM, applicable to current data and future estimates. Findings indicate that beams manufactured solely with wire-arc DED are sensitive to fluctuations in specific environmental impact and cost of wire-arc DED, potentially losing their material saving advantage. Conversely, hybrid beams that combine conventional profiles with wire-arc DED offer a better balance between structural performance, sustainability and economic feasibility.

1. Introduction

Metal additive manufacturing (AM) technology has been developing quickly over the past years and has become a viable method for application in construction [1]. Advancements in wire-arc directed energy deposition (DED) methods have made it possible to print metal parts far exceeding the typical size limits and deposition rates of laser powder bed fusion (LPBF) [2,3]. Material properties of wire-arc DED parts have also been found satisfactory. For example, the Young's modulus and yield stress of wire-arc DED and conventionally made stainless steel used in construction are comparable [4,5]. The fatigue behaviour of wire-arc DED steel is also similar to steel butt welds and S355 structural steel in as-built and machined forms, respectively [6,7]. Several structural prototypes made by wire-arc DED have been illustrated in Fig. 1, such as small- to medium-size pedestrian bridges [8,9], optimised beams and columns [10,11] and complex nodes [12,13]. Special attention is being directed to hybrid manufacturing using wire-arc DED and conventional profiles to strengthen conventional profiles [14–18] and for fatigue repair [19–21]. Further investigation into the wire-arc DED of smart materials is also enabling innovative designs in structural engineering [22–24].

The new possibilities offered by wire-arc DED can accommodate advanced design approaches to harness its full potential, particularly concerning reduced material usage. Topology optimisation (TO), as the most potent approach for optimising structures, usually results in complex geometries that are prohibitively expensive or practically impossible to produce using conventional manufacturing (CM) methods. Wire-arc DED has enabled the production of such complex structures. However, whether the material savings achieved in this way can be translated into lower environmental impact is not a trivial question [25]. Another important consideration is the economic feasibility of wire-arc DED, which becomes especially important in large-scale applications in construction as a low-profit margin industry. Therefore, further investigations are required to investigate its potential for sustainability and cost-competitiveness compared to CM for building structures.

Topology-optimised designs realised by wire-arc DED can offer material savings compared to subtractive manufacturing methods for producing a certain component, as subtractive techniques often generate lots of waste when producing a component from a billet. This efficiency is commonly expressed as the buy-to-fly ratio (equal to the total weight of the billet over the weight of the part) or its inverse, the utilisation factor. These metrics primarily depend on the component's geometrical complexity [26–29]. However, wire-arc DED does not significantly reduce waste compared to formative process such as hot rolling, which typically produces minimal waste is the most relevant CM method for

* Corresponding author.
E-mail addresses: baqershahi@stahl.uni-hannover.de (M.H. Baqershahi), C.Ayas@tudelft.nl (C. Ayas), ghafoori@stahl.uni-hannover.de (E. Ghafoori).

Nomenclature

AM	Additive manufacturing
DED	Directed energy deposition
LPBF	Laser powder bed fusion
TO	Topology optimisation
CM	Conventional manufacturing
LCA	Life cycle assessment
CNC	Computerised numerical control
SIMP	Solid isotropic material penalisation
ρ_e	Density of element e
E_e	Young's modulus of element e
p	Penalty in SIMP method
E_0	Solid Young's moduli
$E_{\min}$	Void Young's moduli
$\widetilde{\rho}_e$	Filtered density of element e
v_i	Volume of element i
w_{ie}	Weighting factor between elements i and e for filtering scheme
$r_{\min}$	Filtering radius
Δ_{ei}	Distance between elements i and e
$\widetilde{\widetilde{\rho}}_e$	Projected density of element e
μ	Projection threshold
β	A coefficient controlling the sharpness of the Heaviside function
V	Volume of the structure
$\mathbf{K}$	Global stiffness matrix of the structure
$\mathbf{u}$	Vector of nodal displacements
$\mathbf{f}$	Vector of nodal forces
c	Compliance of the structure
c_0	Maximum allowable compliance
V^{dil}	Volume of the dilated field
c^{ero}	Compliance of the eroded field
c^{int}	Compliance of the intermediate field
MMA	Method of moving asymptotes
I	Environmental impact of a structure
a_M	Specific environmental impact of a construction method M for a unit of volume
b_M^*	Specific variable cost of a construction method M for a unit of volume
b_M	Specific equivalent total cost of a construction method M for a unit of volume
C_i^{fixed}	Fixed costs associated with manufacturing of a component i
$C_i^{variable}$	Variable costs associated with manufacturing of a component i
C	Total cost of a component
r_e	Normalised environmental impact ratio of wire-arc DED to CM
r_c	Normalised cost ratio of wire-arc DED to CM
FOB	Fully-optimised beam
HYB	Hybrid beam

---

construction applications, as shown in Fig. 2.

However, by employing TO to reduce weight while maintaining the desired performance, wire-arc DED could gain an advantage over hot rolling, which is much more restricted in terms of form freedom, as schematically illustrated in Fig. 3. Nevertheless, it cannot be taken for granted that a 1:1 relation between weight reduction and environmental impact exists [25].

There are a few studies that have simultaneously considered TO and sustainability, albeit from different perspectives. For instance, a feature-based level set concept was introduced to enable remanufacturing of a component at the end of its life through subtractive machining into another lower-level model within the same product family [30]. Another sustainability-oriented optimisation framework includes an inner level that performs the common TO and an outer loop using a generative framework to improve the sustainability of the design [31]. This is achieved by minimising an objective function composed of a weighted sum of several criteria, including a sustainability index. Additionally, multi-material TO, which combines steel with low-impact biomaterials, has been another strategy to incorporate sustainability into design optimisation [32]. For example, efforts have been made to minimise support volume and surface area alongside compliance [33,34]. Multi-material approach has been also utilised to balance performance and cost [35]. While each work offers valuable insights, it is crucial to have a closer look at the environmental and economic impact of wire-arc DED in the context of construction industry to establish suitable strategies.

1.1. Sustainability of wire-arc DED

According to the life cycle assessment (LCA) studies on wire-arc DED of structural steel, summarised in Table 1, the initial material production constitutes the highest share of the environmental impact for the production of a component. To further clarify this, the production steps from cradle to gate for wire-arc DED and hot rolling are demonstrated in Fig. 4.

It should be noted that the term "hot rolling" is used in two contexts:

1) as the conventional method for producing of standard profiles in construction; and 2) as a production step common to both CM and wire-arc DED. Obviously, wire-arc DED approach involves two extra steps of wire drawing and deposition process compared to CM. This leads to increased energy consumption and production costs per unit of weight. Consequently, wire-arc DED has a higher specific environmental impact and cost, as reported in various case studies [28,36]. Fig. 5 demonstrates an estimation of the specific environmental impact of wire-arc DED and hot rolling to produce 1 kg of carbon steel and stainless steel based to the previous LCA studies [29,37]. The carbon emissions associated with wire-arc DED of stainless steel and carbon steel are approximately 1.66 and 2.5 times greater than hot rolling. In fact, the only study that specifically compared the environmental impact of a wire-arc DED beam and a hot-rolled beam in construction concluded that at least 50 % material saving for a wire-arc DED beam is required to be more sustainable than a hot-rolled beam [36]. This suggests that the specific environmental impact in terms of carbon emission for wire-arc DED is about twice as high as that of CM.

1.2. Economic potential of wire-arc DED

Many studies have investigated the cost estimation of AM methods, such as the one in reference [41]. However, the first publication specifically addressing the cost estimation of wire-arc DED was released in 2015 by Martina and Williams, in which wire-arc DED was found to offer cost savings between 7 and 69 % over machining for the production of titanium parts [42]. Several other cost evaluations of wire-arc DED of titanium components also confirmed its cost-effectiveness compared to machining methods [43,44]. However, studies on the cost of wire-arc DED of steels, which are typically used in construction, are much less prevalent, as summarised in Table 2.

These studies compared wire-arc DED of steel with either CNC or LPBF of steel, but there is no consensus among them on the cost breakdown of wire-arc DED. Different studies identified various main cost drivers, such as materials and consumables, deposition process,
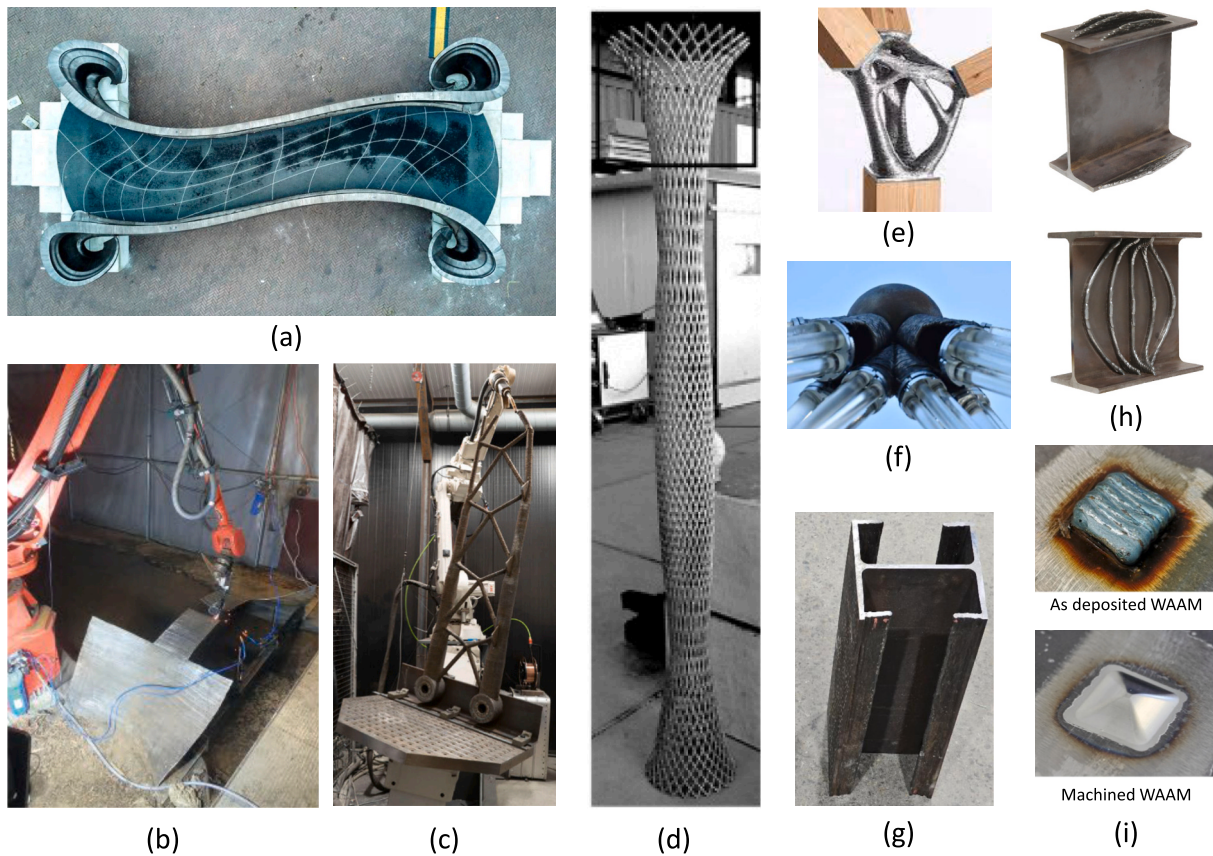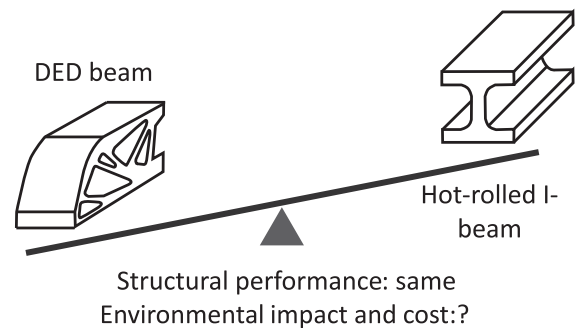
Fig. 1. Examples of using wire-arc DED for construction applications (a) MX3D pedestrian bridge in Amsterdam [8], (b) in-situ printed footbridge in Darmstadt [9], (c) cantilever truss beam [10], (d) diagrid column [11], (e) joint connection in a timber structure [12], (f) joint connection in a glass structure [13], (g) strengthening of I-profile column [15], (h) local strengthening of I-profile [14], (i) local fatigue strengthening [20].
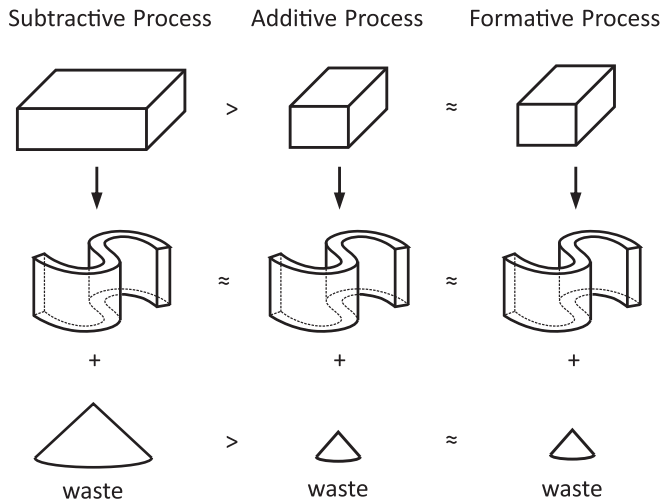
Fig. 2. Comparison of subtractive, additive and forming manufacturing methods in terms of produced waste for manufacturing of a given component.

Fig. 3. Material saving potential of wire-arc DED over hot-rolling through topology optimisation.

labour and post-processing. For instance, the share of material and consumables from the total cost was reported to be between 4 and 84 %. This variation could be attributed to various underlying assumptions in each study. Nonetheless, it can be interpreted that the cost and the mass of a component are directly or indirectly correlated. For example, material costs are directly linked to the total cost, while the deposition process or labour costs are associated with time, which is itself related with the mass of the structure. As shown in Fig. 4, it is reasonable to

assume that the specific cost of wire-arc DED is higher than hot rolling due to the extra production steps involved, so a certain amount of material saving is required for wire-arc DED to be cost-effective compared to CM.

1.3. Scope of the study

Reviewing the existing literature reveals a notable gap in incorporating sustainability and cost aspects at the conceptual design stage for optimised large-scale structures intended for manufacturing with wire-arc DED. LCA and cost modelling studies are often confined to pre-defined boundaries and typically lack a comprehensive approach to redesigning and optimisation of components. Although some studies considered redesigning thorough optimisation, these efforts are often

Table 1
LCA Studies on wire-arc DED of steel.

Material	Compared with	Functional unit	Findings	Study
Stainless Steel (308I)	Casting CNC milling	Mass-based	• Wire-arc DED has a comparable environmental impact with green sand casting and CNC (with a utilisation factor of 0.75). • The main contributing factor to environmental impact is raw material production, and it has a linear relation with the weight. • Material savings offered by wire-arc DED provide an opportunity to reduce its environmental impact.	[29]
Structural Steel (EN S235JR)	machining	blade	• A considerable share of the total required energy for wire-arc DED is attributed to the pre-manufacturing step (more than 20 %), except for raw material production. • With the integration of wire-arc DED and subtractive method significant savings in material (60 %) and energy (34 %) are possible compared to machining.	[38]
Aluminium, Titanium, Steel (ER70)	Machining	Frame, bracket, beam	• Energy and CO2 emissions are dominated by material production. • Wire-arc DED provides a significant reduction in energy demand and CO2 emission compared to machining. • Time and cost associated with wire-arc DED depend on the material and exhibit different trends.	[37]
Stainless Steel (316 L)	Machining	A given component	• The main contributions to the environmental impact of wire-arc DED come from material production followed by electricity and shielding gas. • Environmental benefits of wire-arc DED are due to lower material waste compared to machining. This study considered two buy-to-fly ratios of 3.2 and 1.2 for rough and fine machining, respectively.	[39]
Steel (ER70)	CNC milling	Gear, cylinder and a S-shaped geometry	• Wire-arc DED has a lower environmental impact than CNC due mainly to lower material removal/waste. • The highest and lowest contributions to the total environmental impact are associated with steel billet production and the hot-rolling process (the step before wire drawing), respectively. • The main advantage of wire-arc DED lies in its potential to save material. At least 50 % weight saving is needed for wire-arc DED to have a smaller carbon footprint than CM.	[27]
Carbon Steel (S355), Stainless Steel (304)	Hot rolling	Simply supported beam	• The environmental impact of producing stainless steel is higher than that of carbon steel, which does not reflect its long-term advantages. • Steel production and deposition processes are two main contributors to climate change. Shielding gas has more impact than electricity in the wire-arc DED process. • Potentials to reduce the environmental impact of wire-arc DED process are: using higher deposition rates to reduce gas and energy consumption, as well as renewable energy sources.	[36]
Steel (ER70)	LPBF and CNC	Wall	• CNC with a 50 % material efficiency is more sustainable than wire-arc DED and LPBF. • For higher geometrical complexity and lower material efficiency of CNC, wire-arc DED can outperform it. • The highest share of the environmental impact of wire-arc DED and CNC is related to raw material production, and it also has the highest sensitivity to this factor. For LPBF the highest share and highest sensitivity are related to electricity consumption. • Wie-arc DED found to be slightly better than CNC in terms of environmental impact, owing to its better material efficiency, and more than 4 times better than LPBF thanks to its superior energy efficiency.	[26]
Steel (ER70)	LPBF and CNC	A mechanical part	• Three main contributors to the environmental impact of the wire-arc DED are: steel billet 51 %, shielding gas 20 %, and post processing 13 %. Hot rolling and wire drawing together constitute 9 % of the total impact. • The main ecological burden of CNC stems from steel billet (75 %) and electricity (19 %). For LPBF, three main contributions come from electricity (36 %), inert gas (26 %), and gas atomisation (23 %). • Wire-arc DED is more sustainable than both CNC and LPBF in almost all LCA measures.	[40]
Steel (ER70)	LPBF and CNC	Marine propeller	• The key contributor to the environmental impact of wire-arc-DED and CNC is primary material production, while for LPBF, the consumed energy during the process has the highest contribution. • Wire-arc DED has a higher specific environmental impact and, therefore, can be more sustainable only when its material savings are large enough to compensate for its excessive impact. • The environmental impact of consumed energy can be considerably reduced by using renewable energy sources for all of the manufacturing methods.	[28]

conducted in isolation, focusing solely on structural aspects, such as weight minimisation. Most existing studies also assume that an optimised structure is intended for full manufacturing with wire-arc DED.

The present study focuses on integrating sustainability and cost considerations in the conceptual design of structures through TO, rather than aiming for final, ready-to-manufacture designs. This approach involves certain simplifications, such as those related to material properties, structural design criteria, and environmental and economic assessments. Despite the high level of uncertainty during the early design phase, the considerable design freedom available at this stage offers a greater influence on environmental impact [45] and associated

costs. To account for uncertainties in determining the exact environmental impact and cost of wire-arc DED and CM, a comparative parametric framework is utilised to capture the variability and provide generality. Comprehensive LCA and cost evaluations, which require detailed information, typically become feasible only at later stages when opportunities for modifications and changes are much reduced.

Despite its importance, detailed considerations of manufacturing aspects, such as the choice of deposition strategy, heat management and the resulting residual stresses and distortions, are not considered in this study. Numerous studies suggested approaches to integrate certain manufacturing constraints into TO, such controlling overhangs [46,47]
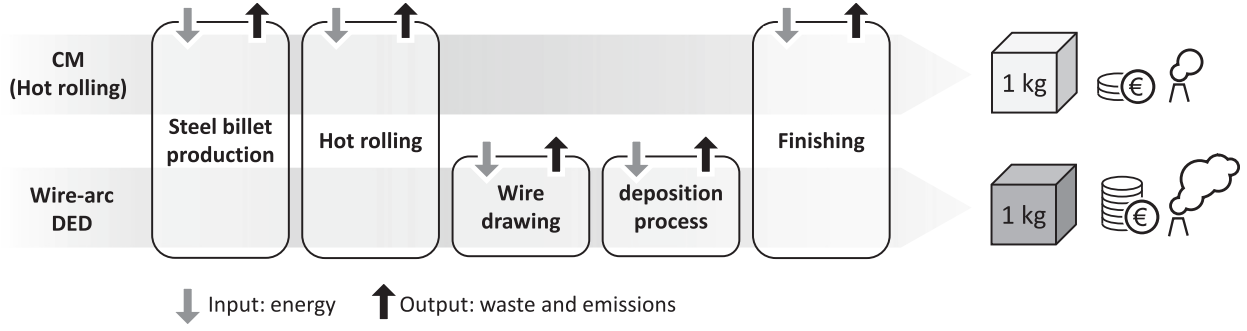
Fig. 4. Main production steps of hot rolling and wire-arc DED. Producing 1 kg of material with wire-arc DED involves extra steps that increase energy consumption and costs.
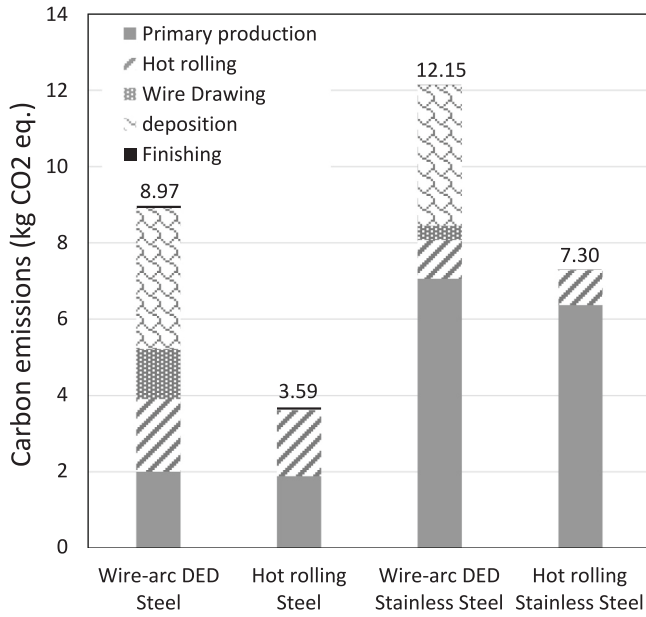

Fig. 5. Carbon emissions associated with producing 1 kg of material by wire-arc DED and hot rolling, adapted from [29,37].

and managing geometrical complexity [48]. However, overhangs are less problematic in DED compared to PBF due to greater freedom in build direction. Geometrical complexity can also be managed through length scale control strategies, as demonstrated in this study.

2. Methodology

In this study, density-based TO with solid isotropic material with penalisation (SIMP) interpolation law [49] is used as the computational design tool suitable for production with AM. The TO results are integrated with predictive models for environmental impact and cost, and a parametric study is conducted to examine the sustainability of fully optimised, hybrid and conventionally manufactured structures. Two length scale control strategies are investigated for TO and their effects are analysed and compared. Particular emphasis is placed on the potential of combining standard profiles with wire-arc DED for improved sustainability and economic viability.

2.1. Topology optimisation

The design domain for TO is divided into N finite elements, each with a design variable pseudo density of ρ_e that ranges from 0 to 1 corresponding to void and solid, respectively. The Young's modulus of an

element is determined as:

$$E_e(\rho_e) = E_{\min} + \rho_e^{\,p}(E_0 - E_{\min}), \tag{1}$$

in which $E_{\min} = 1 \times 10^{-9}$ and $E_0 = 1$ are the void and solid moduli, respectively, and p is the penalisation exponent taken as 3. Due to the well-known numerical instabilities associated with the SIMP method, such as mesh-dependency and formation of checkerboard patterns [50], a convolution filter following Bruns and Tortorelli [51] is applied on the ρ field where $\widetilde{\rho}_e$ is the filtered density associated with the element e which is defined as:

$$\widetilde{\rho}_e = \frac{\sum_{i=1}^{N} w_{ei} v_i \rho_i}{\sum_{i=1}^{N} w_{ei} v_i}, \tag{2}$$

where

$$w_{ei} = \max(0, r_{\min} - \Delta_{ei}), \tag{3}$$

where $r_{\min}$ is the radius over which filtering is applied and also controls the minimum size of solid features. Δ_{ei} represents the distance between the elements e and i. Additionally, a projection scheme is used to achieve sharp black-and-white designs from the filtered field with grey regions. For this purpose, a smooth Heaviside function is considered as follows [52]:

$$\overline{\widetilde{\rho}}_e = \frac{\tanh(\beta\mu) + \tanh\left(\beta\left(\widetilde{\rho}_e - \mu\right)\right)}{\tanh(\beta\mu) + \tanh(\beta(1 - \mu))}, \tag{4}$$

where $\overline{\widetilde{\rho}}_e$ is the projected density, μ is the threshold limit between 0 and 1 above which the density is mapped close to 1 and otherwise close to 0, and β is the parameter controlling the sharpness of the Heaviside function. Starting with $\beta = 1$, the value of β is increased gradually at certain design iterations to approach a sharp Heaviside function.

Applying a convolution filter followed by a projection scheme can impose minimum length scale control on the void regions when μ is set to 1 and on solid regions when μ is set to 0. Robust formulation proposed by Wang et al. [52] provides the possibility to impose minimum length scale control on both void and solid regions, while ensuring robustness against manufacturing errors. In both cases, the resulting imposed minimum length scale can be related to projection threshold and the minimum filter radius and projection threshold. For a given projection threshold, choosing a small filter radius result in intricate designs that might be challenging to manufacture and, more importantly, more sensitive to geometrical deviations. A larger filter radius yields simpler designs with bulkier elements and heavier designs for a given compliance but is principally less sensitive to geometrical inaccuracies. In addition to controlling the manufacturability of the designs, minimum length scale control of solid regions also affects the susceptibility of the elements to buckling. While robust formulation imposes an extra restriction to the design domain, namely minimum length scale control on

Table 2-
Summary of cost estimation for wire-arc DED of steels.

Material	Compared with	Functional unit	Findings	Study
Aluminium, Titanium, Steel (ER70)	Machining	Frame, bracket, beam	• Wire-arc DED is more expensive than machining to produce steel beam. • The cost breakdown of wire-arc DED is approximately: 87 % deposition process, 11 % machining and < 1 % feedstock material. • Wire-arc DED has a lower cost than the subtractive method, and retains its advantage for different annual batch sizes, demonstrating its potential mass production.	[37]
Stainless Steel (316 L)	Machining	A given component	• The cost breakdown of wire-arc DED excluding machining is: 84 % material and consumables, 7 % equipment, 5 % labour, 3 % overhead, <1 % energy. • Variable costs show the highest sensitivity to wire feedstock price, while fixed costs have the highest sensitivity to machine uptime and machining equipment.	[39]
Steel (ER70)	LPBF and CNC	Marine propeller	• Wire-arc DED has the lowest production cost, followed by CNC, both of which cost much less than LPBF. • The cost breakdown of wire-arc DED is: 66 % post-processing, 16 % labour, 12 % machine, 5 % material and 1 % consumables. • For simple and complex geometries, CNC (with 50 % material efficiency) and wire-arc DED are the cheapest, respectively. Material efficiency of around 11 % is the breakeven point of CNC with wire-arc DED.	[28]
Steel (ER70)	LPBF and CNC	Wall	• The main cost drivers of all methods are labour and machine costs. The highest cost sensitivity was concerning process time, followed by labour and machine costs. • The cost breakdown of the wire-arc DED component reads as: 44 % labour, 35 % machine, 14 % post-processing, 6 % material and < 1 % consumables.	[26]

void regions, it is not obvious how this would affect the designs and, subsequently, their economic and environmental assessments of the designs. Therefore, both approaches are considered in this study.

2.1.1. Minimum length scale control through convolution filter and projection

Applying a convolution filter followed by a projection that ensures crisp solid-void designs enables imposing an exact minimum length scale on the solid regions, as demonstrated in Fig. 6. For instance, with a projection threshold of $\mu = 0.5$, the imposed minimum length scale can be estimated as $L_{\min} = 0.28 \times 2r_{\min} = 0.56r_{\min}$.

Aiming to design structures with a certain structural performance, namely compliance as a measure of global stiffness, the optimisation problem is defined as the minimisation of the volume V subjected to compliance constraint c_0 that is formulated as:

$$\begin{aligned} &\min_{\rho} V \\ &\text{subject to} \\ &0 \leq \rho \leq 1 \\ &\mathbf{K}\mathbf{u} = \mathbf{f} \\ &c \leq c_0, \end{aligned} \tag{5}$$

in which $\mathbf{K}$ is the stiffness matrix of the structure, $\boldsymbol{\rho}$, $\mathbf{u}$, $\mathbf{f}$ are the arrays containing the density of elements, nodal displacements and applied forces, respectively, and $c = \mathbf{f}^{\mathrm{T}}\mathbf{u}$ is the compliance of the structure. Both volume and compliance are calculated based on the projected density field.

2.1.2. Minimum length scale control through robust formulation

Robust formulation has been originally introduced to provide desired minimum length scale control on both solid and void regions. It not only prevents the formation of sharp edges that are not desirable for manufacturing but also provides robustness against possible manufacturing errors, namely under- and over-etching. Robust formulation consists of three sets of distinct projections applied to the filtered field that represent under-etched, intended-to-manufacture, and over-etched fields. These fields are labelled as eroded, intermediate and dilated and are defined so that $0 < \mu^{\mathrm{dil}} < \mu^{\mathrm{int}} < \mu^{\mathrm{ero}} < 1$, as schematically shown in Fig. 7. Robustness is achieved by applying a min-max formulation to optimise the objective function for the worst case, which is the eroded field for the compliance problem. The threshold for the intermediate field is usually set at 0.5, while dilated and eroded

thresholds are usually considered symmetric with respect to the intermediate field unless there is a specific requirement to consider otherwise. In this study, 0.25 and 0.75 are selected for μ^{dil} and μ^{ero} respectively.

In the case of robust formulation, the optimisation problem is defined as:

$$\begin{aligned} &\min_{\rho} V^{\mathrm{dil}} \\ &\text{subject to} \\ &0 \leq \rho \leq 1 \\ &\mathbf{K}\mathbf{u} = \mathbf{f} \\ &c^{\mathrm{ero}} \leq c_0^{\,*}, \end{aligned} \tag{6}$$

where V^{dil} is the total volume of the dilated field and c^{ero} is the compliance of the eroded field. The choice of dilated volume instead of intermediate volume for the objective function only provides numerical stability and convergence [52]. While compliance constraint has to be applied to the eroded field for the sake of robustness, the intended design for manufacturing is the intermediate field. Therefore, the constraint limit $c_0^{\,*}$ should be updated at certain intervals, in this study at each iteration, by a factor of $c^{\mathrm{ero}}/c^{\mathrm{int}}$ to ensure that the desired compliance constraint for the intermediate field is met. The minimum length scale control on both solid and void regions achieved by robust formulation can be estimated according to Fig. 8. For example, the choice of $\mu^{\mathrm{dil}} = 1 - \mu^{\mathrm{ero}} = 0.25$ imposes $L_{\min} = 1 \times 2r_{\min} = 2r_{\min}$.

The 3D TO implementation in MATLAB by Ferrari and Sigmund [53] is used in this study, together with the method of moving asymptotes as the optimiser [54]. Initialised at 1.0, the value of β is increased by 1.5 times at every 30 iterations to a maximum of 38. Maximum iteration number of 400 and a minimum change of filtered density's norm equal to 1×10^{-6} are two stopping criteria.

2.2. Environmental and economic assessment

The environmental impact is often described using a wide range of impact categories, such as climate change and human toxicity. Midpoint indicators are the measures used to represent the impact on each of these impact categories at a midway point in the cause-effect chain [55]. The evaluation of midpoint categories can be achieved by undertaking a comprehensive LCA, which involves a detailed definition of system boundaries and collection of inventory data.

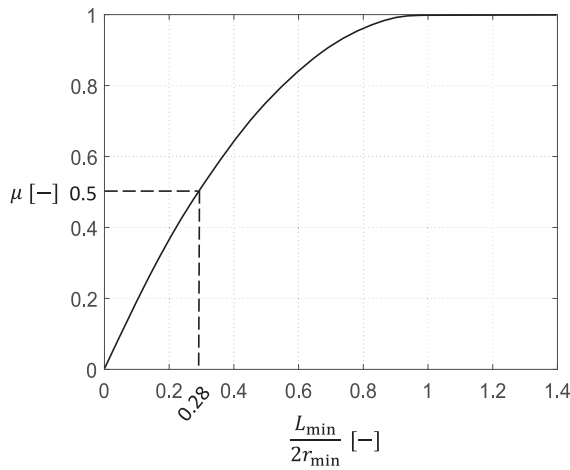Based on the previous LCA studies presented in Table 1, particularly

Fig. 6. Relation between normalised minimum length scale and a Heaviside projection with a threshold of μ [52].
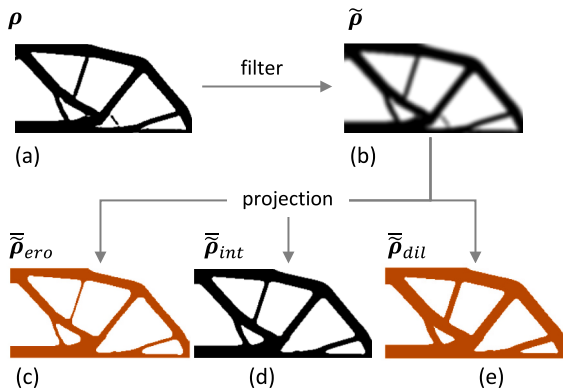

Fig. 7. Filtering and projection schemes, (a) initial density field ρ, (b) filtered density field $\tilde{\rho}$, (c) eroded (or under-etched) density field $\bar{\bar{\rho}}_{ero}$ resulted from projecting the filtered field with a threshold of $\mu^{ero} = 0.75$, (d) intermediate field $\bar{\bar{\rho}}_{int}$ resulted from projecting a filtered field with a threshold of $\mu^{int} = 0.5$, (e) dilated (or over-etched) field $\bar{\bar{\rho}}_{dil}$ as a result of projecting a filtered field with a threshold of $\mu^{dil} = 0.25$.

the work by Shah et al. [36] (details in the Appendix A, Table A.1), a linear relation between the volume of a component V and its corresponding environmental impact I can be considered as follows:

$$I^{IC} = a_M^{IC} \bullet V, \tag{7}$$

where a_M^{IC} is the specific environmental impact in terms of impact category IC that is associated with a manufacturing method M. The specific environmental impact encapsulates all the other influential factors such production-related parameters.

Following the process-based cost modelling suggested in [39], the total cost can be considered as the sum of variable costs ($C_{variable}$) and fixed costs (C_{fixed}). Variable costs encompass consumable materials, as well as energy and labour that either correlate with the volume directly, or with the time, which is itself a function of volume. Fixed costs depend on many assumptions concerning the production, like machine investment, annual production, design and planning costs, etc. Although fixed costs are principally different from variable costs, it is possible to estimate them as a percentage of variable costs when specific assumptions are made, for instance, as performed by Dias et al. [39]. In this way, the total cost (C) can be estimated as follows:

$$C = C^{variable} + C^{fixed} \cong \left(1 + b_M^*\right) C_{variable} = b_M V, \tag{8}$$
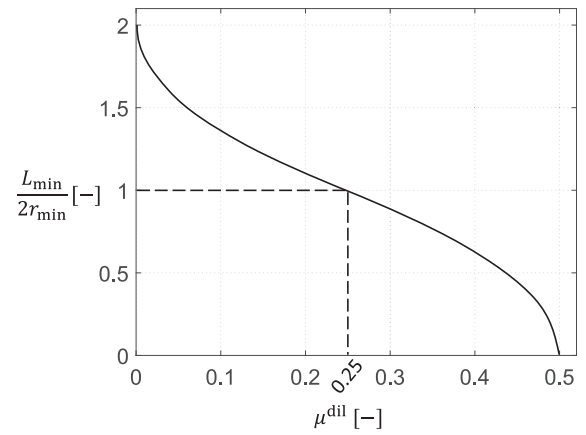

Fig. 8. Relation between normalised minimum length scale and dilated threshold μ^{dil} for a Heaviside projection, assuming that $\mu^{ero} = 1 - \mu^{dil}$ [52].

where b_M^* is the ratio of fixed costs to variable costs for a manufacturing method M, which is obtained after certain assumptions with regard to production are made, for instance, the annual production, yearly maintenance costs, etc. Followingly, the b_M could be determined as the equivalent specific cost of producing a unit of volume.

Based on eqs. (7) and (8), the environmental impact and cost of a hybrid structure that is made with CM and wire-arc DED can be written as:

$$I^{IC} = a_{CM}^{IC} V^{CM} + a_{DED} V^{DED}, \tag{9}$$

$$C = b_{CM} V^{CM} + b_{DED} V^{DED}, \tag{10}$$

in which the volumes produced with CM and wire-arc DED are associated with their corresponding special environmental impact and cost. To conduct a comparative assessment with respect to a reference beam that is made by CM, the environmental impact and cost of lightweight alternatives can be normalised as follows:

$$\frac{I_i^{IC}}{I_{CM}^{IC}} = \frac{a_{CM}^{IC} V_i^{(CM)} + a_{DED}^{IC} V_i^{(DED)}}{a_{CM} \bullet V_{ref}} = \frac{V_i^{CM} + \frac{a_{CM}^{IC}}{a_{DED}^{IC}} V_i^{DED}}{V_{ref}}, \tag{11}$$

$$\frac{C_i}{C_{ref}} = \frac{b_{CM} V_i^{(CM)} + b_{DED} W_i^{(DED)}}{b_{CM} \bullet V_{ref}} = \frac{W_i^{CM} + \frac{b_{DED}}{b_{CM}} V_i^{DED}}{V_{ref}}. \tag{12}$$

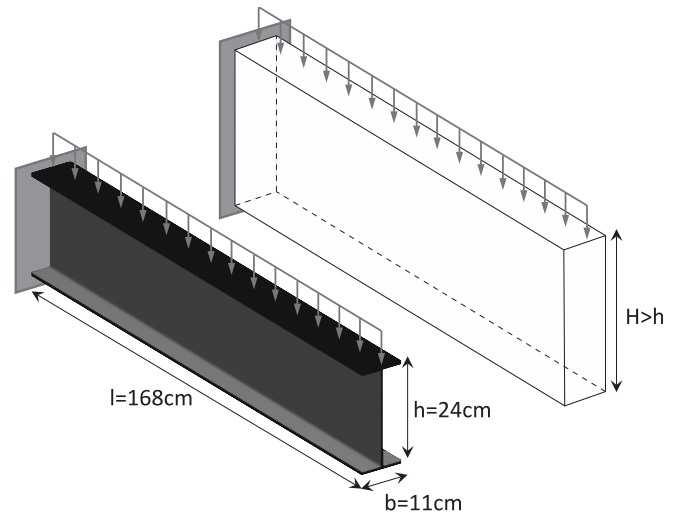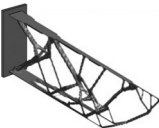Eqs. (11) and (12) show that when the environmental impact and
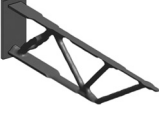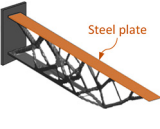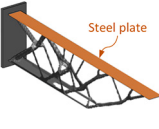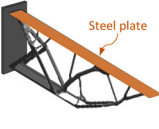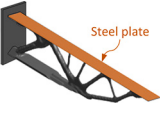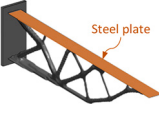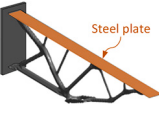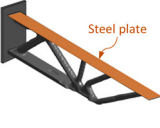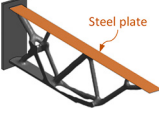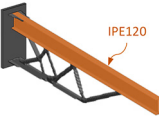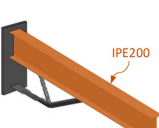
Fig. 9. Reference cantilever I-beam (left), and design domain for TO (right).

Table 3-
Alternative fully optimised beams (FOBs) and hybrid beams (HYBs) with similar structural performance, featuring various heights and imposed minimum length scale.

Alternative (length scale)	Height increase (%)		
	25	50	75
FOB – 1 (rmin = 3 cm)			
FOB – 2 (rmin = 6 cm)			
FOB – 3 (rmin = 3 cm + robust)			
HYB – 1 (rmin = 3 cm)			
HYB – 2 (rmin = 6 cm)			
HYB – 3 (rmin = 3 cm + robust)			
HYB – 4 (rmin = 3 cm)			
HYB – 5 (rmin = 3 cm)			
HYB – 6 (rmin = 3 cm)			

cost are normalised with respect to the reference beam, weight factors $r_e = \frac{a_{CM}^{IC}}{a_{DED}^{IC}}$ and $r_c = \frac{b_{DED}}{b_{CM}}$ emerge that represents the environmental impact and cost ratio of wire-arc DED to CM per unit of weight, respectively. These normalised ratios correspond to the additional specific impact and cost of wire-arc DED compared to CM, as explained in the introduction; thus, both factors are greater than one. Shah et al. reported breakeven point of wire-arc DED beams and conventional I-beams for three impact categories — climate change, human toxicity and metal depletion — at 2, 3.7, and 1.2, respectively. Comparable values can also be obtained from other LCA studies in the range of 1.66 and 2.5 [29,37]. Referring to eq. (11), these breakeven points correspond to r_e. Clearly, this value can vary significantly across different impact categories. Moreover, production-related parameters can have a considerable influence. For

instance, increasing the deposition rate of wire-arc DED process from 0.5 kg/h to 10 kg/h can reduce associated carbon emissions by nearly 66 % [36]. Another example is the proportion of renewable sources in the energy mix; switching from 100 % fossil fuels to 100 % renewables could reduce the environmental impact by 31 % [36]. To account for the uncertainty in determining these factors and represent their variation, a parametric study is conducted. Based on the literature, a window range between 1.0 and 2.0 is considered for this study, focusing primarily on the climate change category (GWP100). In the absence of comparable cost information in the literature, a similar range of 1.0–2.0 for r_c is considered that is expected to be economically relevant. While smaller values, potentially achievable through further technological progress, would further promote the use of wire-arc DED, larger values than three imply that wire-arc DED would not be practically competitive with CM.

Fig. 10. Normalised volume of FOBs and HYBs with respect to the reference beam as a function of height increase in the design domain.

3. Results and discussion

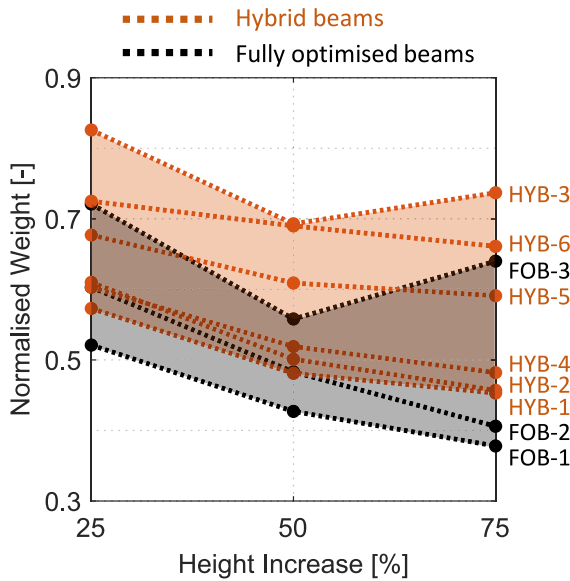In this study, a simple numerical case is analysed to demonstrate how environmental and economic considerations can influence the design and topology optimisation of lightweight structures. To ensure comparability, the same structural performance is considered for all the lightweight designs obtained from TO by setting a compliance constraint that represents the overall stiffness of the structure. A typical structural member, a cantilever I-beam, serves as the reference design, with a distributed load and the dimensions specified in Fig. 9 (left). The geometrical dimensions of the I-beam are chosen to be close to the conventional IPE240. The design domain for TO of lightweight beams is based on the dimensions of the reference beam, while its height is increased by 25 %, 50 %, and 75 % to expand the design freedom. Two types of lightweight beams are designed, namely fully optimised beams (FOBs) and hybrid beams (HYBs). FOBs are designed by exploiting the total design freedom over the design domain. These beams are supposed to be fully manufactured with wire-arc DED. For HYBs, a portion of the design domain is assumed to be fixed and made of a conventional profile. There are many ways to presume a part produced by CM in the design domain. Here, two types of HYBs are considered: (1) a conventional steel plate with a thickness of 1 cm as the top flange of the beam combined with a topology-optimised wire-arc DED profile, and (2) I-beams smaller than the reference beam combined with a topology-optimised wire-arc DED profile. The sizes of these I-beams are chosen to be close to IPE120, IPE160, and IPE200.

For FOBs and HYBs with a steel plate, three different settings for length scale control are considered: (1) small filter radius (r_{min} = 3cm); (2) large filter radius (r_{min} = 6cm) with a minimum length scale on solid region equal to 1.68 and 3.36, respectively; (3) robust formulation with a small filter radius (r_{min} = 3cm) with an imposed minimum length scale on both solid and void regions equal to 6 cm (according to sections 2.1.1 and 2.1.2). HYBs with IPE sections are designed only with a small filter radius (r_{min} = 3cm). These length scales are much larger than the minimum resolution of wire-arc DED, which can be in the order of millimetres [2]. The outcomes of these design alternatives are shown in Table 3 using the isosurface representation.

3.1. Material savings

Fig. 10 presents the volumes of the design alternatives, normalised by the volume of the reference beam. FOBs provide material saving between 38 and 63 %, while HYBs are 30–52 % lighter than the reference beam. For any given height increase and length scale control, HYBs with a steel plate are approximately 1–24 % heavier than their FOB counterparts. Similarly, HYBs with an I-section are 16–75 % than them. This difference indicates to what extent material savings could can be offset because of hybridisation.

Except for the alternatives obtained through robust formulation, namely FOB – 3 and HYB – 3, the volumes of FOBs and HYBs decrease monotonically as the height of the design domain increases. However, by increasing the height from 50 % to 75 %, the volume of these two exceptions increases. This can be attributed to the fact that by expanding the design space, achieving the same stiffness requires less material, leading to the formation of more slender members. These slender members have a higher probability of being removed by the robust formulation to reduce the sensitivity to manufacturing errors, which can lead to settling into a less optimal local solution. This tendency to increase volume could also be expected if buckling constraints were included. Because increasing the height of the design domain would eventually make the buckling of slender elements critical. This scenario illustrates the complex interplay between design constrains and optimisation outcomes when applying robust formulation or considering stability factors that may limit the maximum possible height. Hence, the following comparisons are made for the designs with a 50 % height increase.

Additionally, it is noticeable that the choice of minimum length scale could significantly affect material saving by constraining the design space. Increasing the minimum length scale from 1.68 to 3.36 and 6 cm increases the weight by almost 6 % and 13 %, respectively. For the similar set of length scales, the weight of hybrid beams with a conventional plate increases by 2 % and 10 %. This suggests that the material saving of hybrid beams are less sensitive to the choice of minimum length scale.

3.2. Environmental and economic assessment

Fig. 11 illustrates how variations of the r_e and r_c affect the normalised environmental impact and cost of each design alternative. The subplots are presented in a design space normalised to the reference design for both environmental impact and cost. The white region represents the area where both criteria outperform the reference beam, indicating the ideal position for a design alternative. The light grey areas between 1 and 1.25 show regions where only one of the two criteria outperforms the reference, while the dark grey areas indicate where both criteria perform worse than the reference. Solid shaded areas represent the position of each alternative as r_e and r_c are varied over the selected range of 1 to 2. FOBs and HYBs are shown in black and orange, respectively.

In Fig. 11, it can be observed that the sensitivity of FOBs is generally higher than HYBs, as evidenced by a larger shaded area for FOBs. This indicates that their lightweight advantage can be quickly offset when the normalised environmental impact and cost ratios of wire-arc DED to CM is large. In contrast, HYBs exhibit less sensitivity due to the inclusion of parts made by CM, even though they are heavier than FOBs. Among the HYBs with a CM steel plate, HYB – 3 with robust formulation performs considerably worse than HYB – 1 and HYB – 2. This is due to the additional constraints imposed by robust topology optimisation formulation, which restricts the material savings.

Interestingly, the sensitivity of HYBs with an I-beam is quite small even for r_e and r_c up to 2. This stands for a favourable trade-off between the lower impact of CM and more optimal material distribution enabled by wire-arc DED. By defining the hybrid ratio as the volume of CM over the total volume of the beam, a trend emerges between the hybrid ratio and the sensitivity of the designs, as shown in Fig. 12. This indicates that while incorporating more CM parts into the design increases the weight, it also stabilises the design's environmental and economic performance.

The implication from Fig. 12 suggest that the proportion of the CM
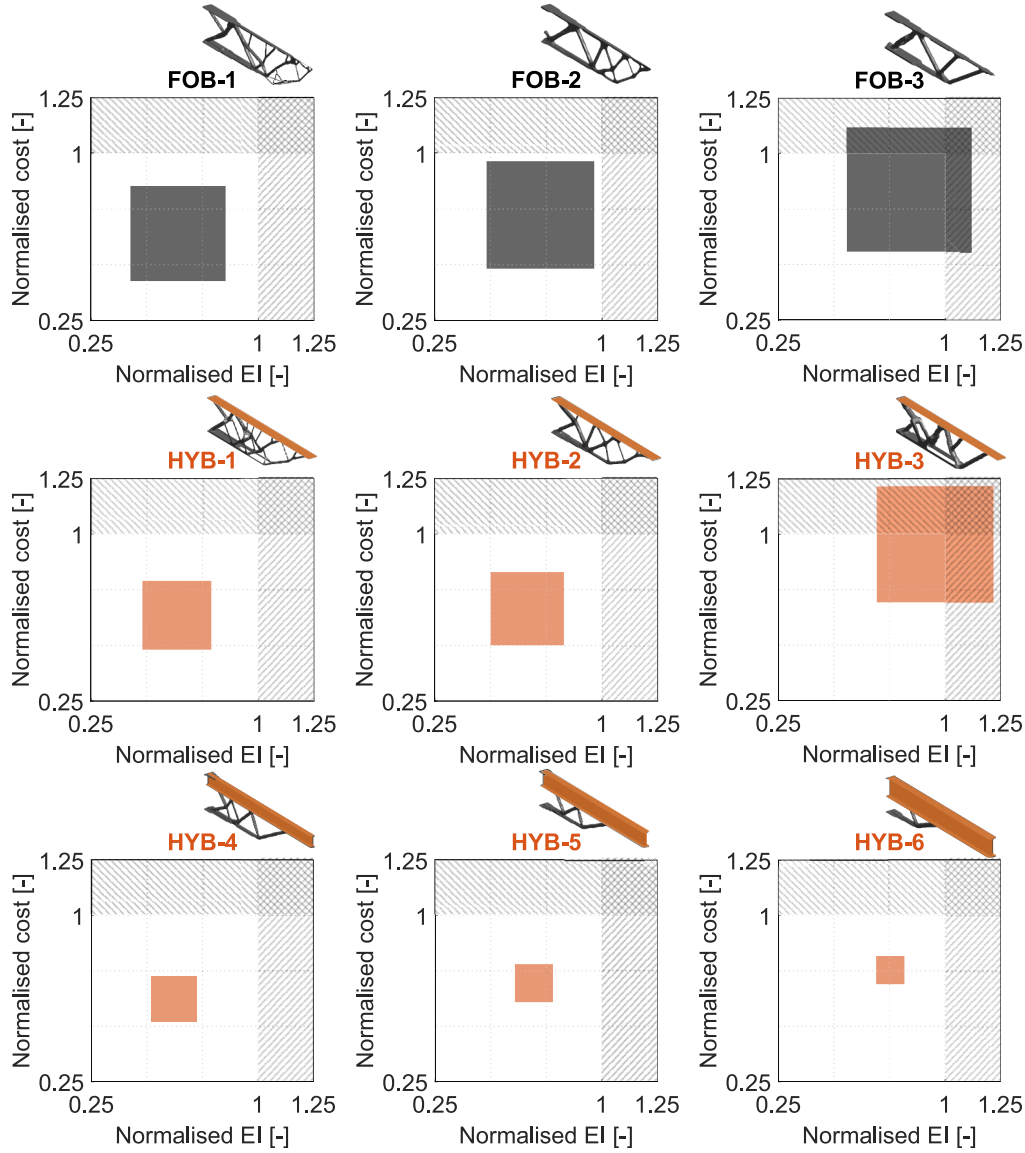
Fig. 11. Variation of normalised environmental impact and cost of alternatives with a 50 % height increase, for r_e and r_c ranging from 1 to 2. The white, light grey, and dark grey areas correspond to regions where both, one, and none of the criteria are superior to the reference beam, respectively. FOBs and HYBs are illustrated in shaded black and orange, respectively. A larger shaded area represents a higher sensitivity of a design to r_e and r_c.

component can play a key role, potentially having greater influence on overall performance than the material savings achieved by TO alone. This insight encourages a reconsideration of design alternatives for further hybridisation by replacing some features obtained from TO, originally intended for wire-arc DED manufacturing with CM profiles. This approach represents a posteriori step, in contrast to the a priori definition of the CM part through the TO, and is only applicable to designs consisting of geometrically simpler, relatively uniform elements. For FOBs, the potential for hybridisation is illustrated in Fig. 13. It can be seen that FOB – 3 obtained through robust formulation, has the greatest potential for substituting the struts with uniform sections, owing to the larger minimum length scale on both solid and void regions. It should be noted that more systematic strategies could be employed for this posterior step, but they were not part of this study.

To present all design alternatives together and clarify the effect of variation of r_e and r_c, as well as the potential of a posteriori hybridisation, Fig. 14 displays nine different scenarios for r_e (increasing from left to right) and r_c (increasing from top to bottom). The post-hybridised version of FOB–3 is denoted by an asterisk.

When $r_e = r_c = 1$ the alternatives are essentially ranked according to

their weights. As either r_e or r_c approaches 2, a Pareto front forms where the FOB-1, FOB-3*, HYB-4 and HYB-5 offer a trade-off between environmental and cost. At $r_e = r_c = 1.5$, several alternatives achieve very close scores, namely HYB – 4, FOB – 3*, HYB – 1 and FOB – 1. As either r_e or r_c approaches 2, FOBs nearly lose their lightweight advantage, and HYB-4 and FOB-3* are the two alternatives with quite close scores, maintaining their lead over other options. This observation aligns closely with the finding by Shah et al. [36], which identifies 50 % material savings (equivalent to $r_e = 2.0$) as the breakeven point for a fully optimised beam made via wire-arc DED compared to a conventional I-beam. The breakeven point of FOB – 3* with the reference beam is approximately at $r_e = r_c = 4.2$.

In summary, while material savings from optimisation give wire-arc DED an advantage over CM, this benefit can be offset by the higher specific environmental impact and cost associated with wire-arc DED. Nonetheless, combining wire-arc DED and CM profiles creates new design possibilities that enhances sustainability and economic feasibility. As explained and demonstrated through a case study, the normalised environmental impact and cost ratios of wire-arc DED to hot rolling are crucial in determining the strategy for design. As long as r_e or
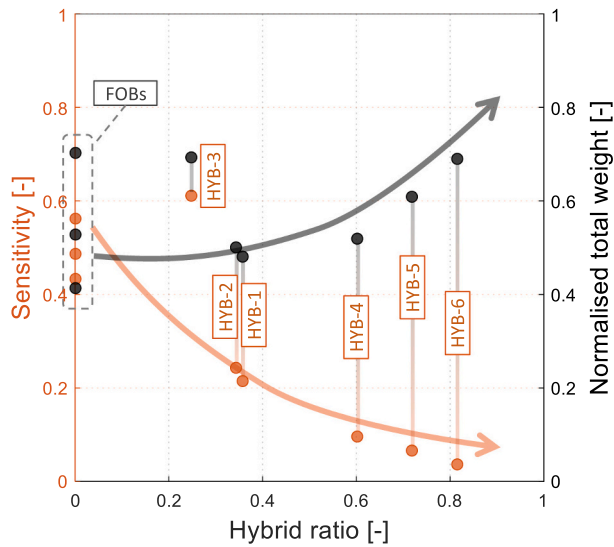
Fig. 12. Normalised weight and sensitivity of the design alternatives as a function of hybrid ratio, defined as the weight of CM part over wire-arc DED part.

r_c are greater than 1, a sustainable and economical design involves a trade-off between the optimal material distribution achievable by wire-arc DED and the low impact, cost-efficient profiles produced by CM. This suggests that a hybrid beam is superior to a fully optimised beam made exclusively by wire-arc DED. In the limiting case of $r_e = 1$ and $r_c = 1$, the total environmental impact and cost of each design would be directly linked to the weight and fully optimised beams would outperform. By assessing fully optimised and hybrid designs over a window range of r_e or r_c, the usability of the methodology and results is ensured when an authoritative opinion emerges about the environmental impact and cost implications of wire-arc DED, providing a design framework to use it for large-scale construction applications economically and sustainably.

3.3. Limitations and outlook

There are certain limitations to this study that, although not affecting the generality of the findings, should ideally be addressed in the future. While a comprehensive structural design involves meeting various limit states with different load cases and combination, this study considered only a single load case and a displacement-related criterion. Incorporating all structural requirements would introduce additional constraints into TO process, likely reducing the material savings further. Moreover, the material properties of steel produced by wire-arc DED and CM were assumed to be identical, although they could have differences that affect the performance of the component. Additionally, the interface of hot-rolled steel and wire-arc DED steel undergoes a special

temperature history that affects its microstructure and can potentially induce residual stresses and distortions. On the other hand, considering manufacturing constraints that were not included in this study is likely to limit the design space even more for TO and offset the material saving potential and favour the hybrid solutions even more. Therefore, setting reasonable expectations regarding the extent of material saving achievable through TO, which is crucial for identifying the breakeven point of wire-arc DED with CM. As technological advancements continue, it is anticipated that both environmental impact and economic feasibility of wire-arc DED will improve. Further experimental investigations in future works remain integral to validating the findings of this study and enhancing the understanding of practical implications, allowing more robust and adaptable design solutions for real-world applications.

4. Conclusions

The paper investigated the environmental and economic potential of wire-arc directed energy deposition (DED) compared with standard profiles made by conventional manufacturing (CM) for construction. Topology optimisation (TO) was used as a computational tool for conceptual design of various lightweight beams. A simplified predictive model for environmental impact and cost was considered, and the methodology was showcased by a case study, comparing conventional I-section beams and optimised lightweight beams. Different minimum length scale controls in TO were considered through filtering and robust formulation. The main variables for the parametric study were the normalised specific environmental impact (r_e) and cost (r_c) ratios of wire-arc DED to CM. The key findings can be summarised as follows:

- The material savings achieved by fully optimised beams and hybrid beams were 38–63 % and 30–52 %, respectively. For any specific minimum length scale control, hybrid beams were 1–75 % heavier than the fully optimised counterparts.
- Increasing the filter radius from 3 cm to 6 cm (corresponding to the minimum length scale of 1.68 and 6 cm) increased the weight of fully optimised beams and hybrid beams between 7.5 and 16 % and 1–6.5 %, respectively.
- While increasing the height of the design domain enables further material savings for a given compliance, there is a limit at which elements become too slender and susceptible to being under-etched during production or buckling.
- The environmental impact and cost of fully optimised beams are more sensitive than hybrid beams to the relative specific environmental impact and cost of wire-arc DED. There is an inverse relationship between the hybrid ratio and how sensitive the design is.
- By imposing minimum length scale control on both solid and void regions, robust formulation tends to produce bulkier elements and simpler geometries compared to just filtering for length scale control. This restrains the material savings in structures, but in addition to
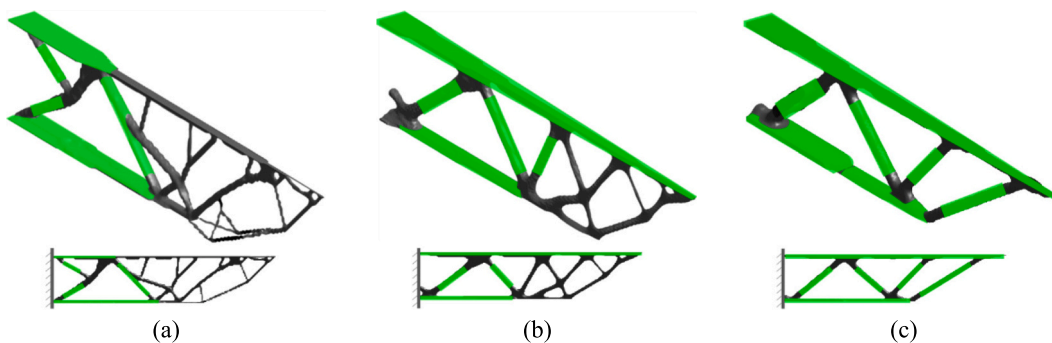
Fig. 13. Posteriori hybridisation of FOBs by considering CM parts where possible: (a) FOB – 1 with around 20 % hybridisation potential, (b) FOB – 2 with around 40 % hybridisation potential, (c) FOB – 3 with around 75 % hybridisation potential, calculated manually by analysing the obtained geometries.
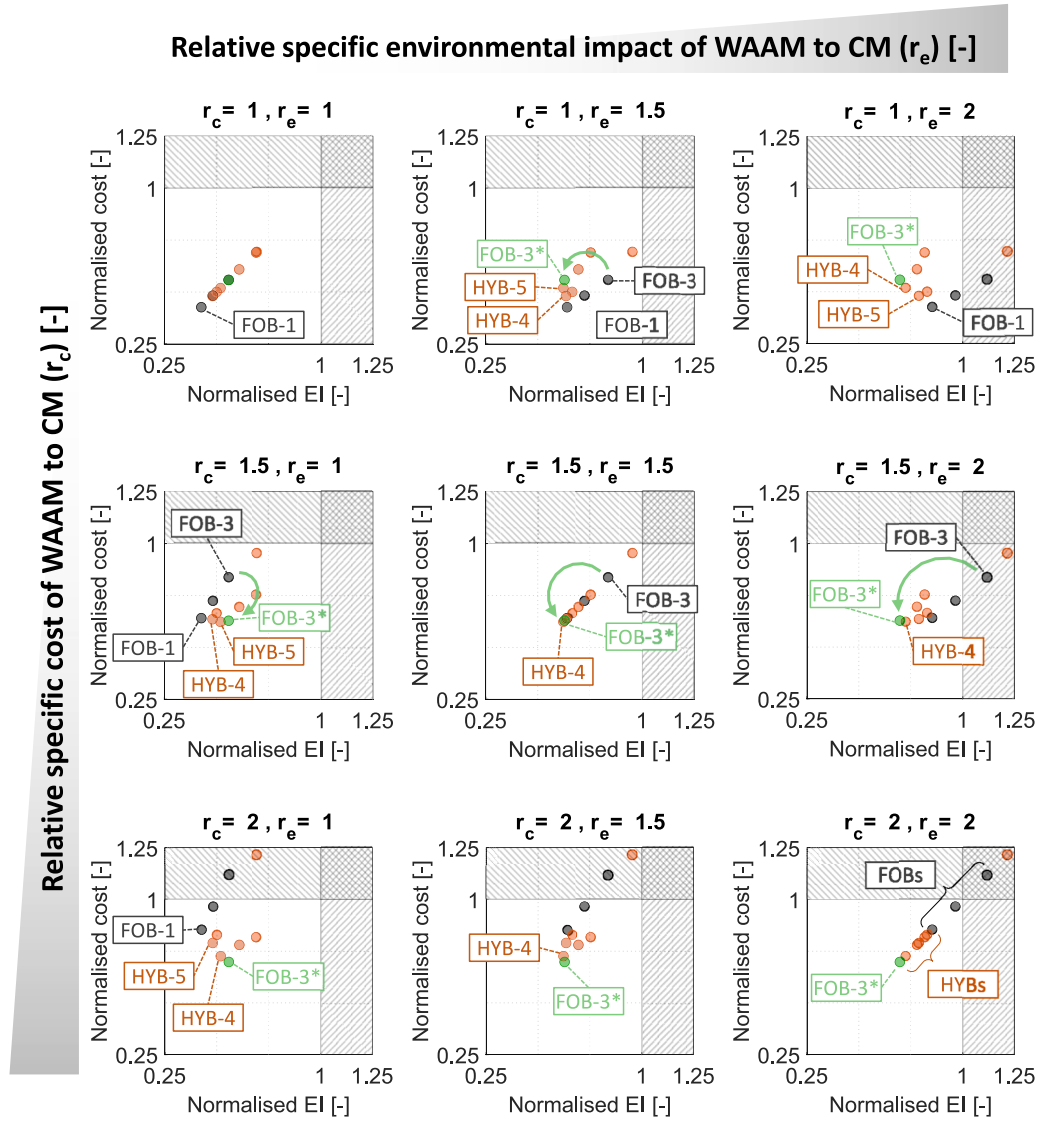
Fig. 14. Parametric study on various normalised environmental impact and cost ratios. Each point represents a design alternative. Horizontal axes and vertical axes show normalised environmental impact and cost, respectively. FOBs (black points) quickly exit the white region where both environmental impact and cost are lower than the reference beam. However, HYBs remain in this region for a wider range of r_e and r_c, despite being heavier than FOBs. Notably, HYBs with a higher share of CM outperform others with smaller shares as the environmental impact and cost increases.

providing robustness against manufacturing errors, the designs are also less sensitive to local buckling and exhibit a higher potential for further hybridisation.

- The breakeven point of fully optimised beams with the reference I-beam in terms of environmental impact and cost is around $r_e = r_c = 2.25$. That of hybrid beams is up to $r_e = r_c = 4.2$, despite weighing more.

This study indicates that due to the trade-off between material savings achievable with wire-arc DED and its higher environmental impact and cost per unit of weight, it cannot be taken for granted that utilising large-scale metal additive manufacturing is necessarily advantageous for structural applications. Moreover, various constraints limit material savings practically achievable thorough topology optimisation. Thus, an effective strategy is likely a hybrid approach using both standard profiles and wire-arc DED, rather than fabricating entire structural components with wire-arc DED alone. Identifying the right share of the conventional profile(s) in the design is not known in advance and depends on the normalised environmental impact and cost ratio of wire-arc DED to CM.

This can be determined through design exploration among viable hybridisation solutions. Nonetheless, an accurate estimation of normalised ratios is necessary for effective decision-making. In a post-hybridisation strategy, on the other hand, larger minimum length scale controls should be used to obtain simpler designs, aiming to use as much standard profiles as possible. The realisation of hybrid solutions can include, for instance, customised new components, strengthening and repair of existing structures, or using wire-arc DED exclusively for complex structural connections.

CRediT authorship contribution statement

Declaration of competing interest

The authors declare that they have no known competing financial interests or personal relationships that could have appeared to influence the work reported in this paper.

Appendix A

In this section, part of a comprehensive LCA study conducted by Shah et al. [36] is provided that compares midpoint impact of wire-arc DED beams to those of conventional I-beams for differential hypothetical mass-ratios. By examining any impact category in this table, it can be verified that the environmental impact is linearly dependent on the mass of wire-arc beam while the system boundaries and the inventory data are constant.

Table A.1
Midpoint impact results for wire-arc DED beams for various hypothetical mass compared to conventional I-beams [36].

Impact category	Unit	I-beam to wire-arc DED beam mass ratio			
		1:01	1.5:1	3:01	4:01
Agricultural land occupation	m2a	0.417	0.278	0.139	0.104
Climate change (GWP100)	kg CO2-eq.	232	155	77.4	58.1
Fossil depletion	kg oil-eq.	66.9	44.6	22.3	16.7
Freshwater ecotoxicity	kg 1,4-DCB-eq.	3.54	2.36	1.18	0.885
Freshwater eutrophication	kg P-eq.	0.127	0.0848	0.0424	0.0318
Human toxicity	kg 1,4-DCB-eq.	137	91.4	45.7	34.3
Ionising radiation	kBq U235-eq.	54.2	36.1	18	13.5
Marine ecotoxicity	kg 1,4-DCB-eq.	4.39	2.93	1.46	1.09
Marine eutrophication	kg N-eq.	0.487	0.324	0.162	0.122
Metal depletion	kg Fe-eq.	74	49.7	24.7	18.5
Natural land transformation	m2	0.0423	0.0282	0.0141	0.0106
Ozone depletion	kg CFC-11-eq.	1.82E-05	1.20E-06	5.99E-06	4.49E-06
Particulate matter	kg PM10-eq.	0.771	0.514	0.257	0.193
Photochemical oxidant	kg NMVOC	0.857	0.571	0.286	0.214
Terrestrial acidification	kg SO2-eq.	0.921	0.614	0.307	0.23
Terrestrial ecotoxicity	kg 1,4-DCB-eq.	0.215	0.143	0.0715	0.0537
Urban land occupation	m2a	1.58	1.05	0.525	0.394

Data availability

Data will be made available on request.

References

[1] L. Gardner, Metal additive manufacturing in structural engineering – review, advances, opportunities and outlook, Structures 47 (2023) 2178–2193, https://doi.org/10.1016/j.istruc.2022.12.039.

[2] S.W. Williams, F. Martina, A.C. Addison, J. Ding, G. Pardal, P. Colegrove, Wire + arc additive manufacturing, Mater. Sci. Technol. 32, H. 7 (2016) 641–647, https://doi.org/10.1179/1743284715Y.0000000073.

[3] A. Taşdemir, S. Nohut, An overview of wire arc additive manufacturing (WAAM) in shipbuilding industry, Ships Offshore Struct. 16, H. 7 (2021) 797–814, https://doi.org/10.1080/17445302.2020.1786232.

[4] P. Kyvelou, H. Slack, D. Daskalaki Mountanou, M.A. Wadee, T.B. Britton, C. Buchanan, L. Gardner, Mechanical and microstructural testing of wire and arc additively manufactured sheet material, Mater. Des. 192 (2020), https://doi.org/10.1016/j.matdes.2020.108675. S. 108675.

[5] V. Laghi, M. Palermo, L. Tonelli, G. Gasparini, L. Ceschini, T. Trombetti, Tensile properties and microstructural features of 304L austenitic stainless steel produced by wire-and-arc additive manufacturing, Int. J. Adv. Manuf. Technol. 106 (2020) 3693–3705, https://doi.org/10.1007/s00170-019-04868-8, 9–10, S.

[6] C. Huang, L. Li, N. Pichler, E. Ghafoori, L. Susmel, L. Gardner, Fatigue testing and analysis of steel plates manufactured by wire-arc directed energy deposition, Additiv. Manufact. 73 (2023) 103696, https://doi.org/10.1016/j.addma.2023.103696.

[7] C. Huang, Y. Zheng, T. Chen, E. Ghafoori, L. Gardner, Fatigue crack growth behaviour of wire arc additively manufactured steels, Int. J. Fatigue 173 (2023) 107705, https://doi.org/10.1016/j.ijfatigue.2023.107705.

[8] L. Gardner, P. Kyvelou, G. Herbert, C. Buchanan, Testing and initial verification of the world's first metal 3D printed bridge, J. Constr. Steel Res. 172 (2020) 106233, https://doi.org/10.1016/j.jcsr.2020.106233.

[9] T. Feucht, B. Waldschmitt, J. Lange, M. Erven, Additive manufacturing of a bridge in situ in: steel construction 15, Nr 2 (2022) 100–110, https://doi.org/10.1002/stco.202100045.

[10] J. Ye, P. Kyvelou, F. Gilardi, H. Lu, M. Gilbert, L. Gardner, An end-to-end framework for the additive manufacture of optimized tubular structures, IEEE Access 9 (2021) 165476–165489, https://doi.org/10.1109/ACCESS.2021.3132797.

[11] V. Laghi, M. Palermo, G. Gasparini, T. Trombetti, Computational design and manufacturing of a half-scaled 3D-printed stainless steel diagrid column 2214-8604 36 (2020) 101505, https://doi.org/10.1016/j.addma.2020.101505.

[12] MX3D (2019) Connector for Takenaka [online]. https://mx3d.com/industries/construction/connector-for-takenaka/ [Access 3. Aug. 2023].

[13] A.H. Snijder, L.P.L. van der Linden, C. Goulas, C. Louter, R. Nijsse, The glass swing: a vector active structure made of glass struts and 3D-printed steel nodes, Glass Struct. Eng. 5 (2020) 99–116, https://doi.org/10.1007/s40940-019-00110-9. H. 1, S.

[14] H. Kloft, L.P. Schmitz, C. Müller, V. Laghi, N. Babovic, A. Baghdadi, Experimental application of robotic wire-and-arc additive manufacturing technique for strengthening the I-beam profiles, Buildings 13, Nr. 2 (2023) 366, https://doi.org/10.3390/buildings13020366.

[15] L. Gardner, J. Li, X. Meng, P. Huang, P. Kyvelou, I-section steel columns strengthened by wire arc additive manufacturing - concept and experiments, Eng. Struct. 306 (2024) 117763, https://doi.org/10.1016/j.engstruct.2024.117763.

[16] J. Yang, M.A. Wadee, L. Gardner, Strengthening of steel I-section beams by wire arc additive manufacturing — concept and experiments, Eng. Struct. 322 (2025) 119113, https://doi.org/10.1016/j.engstruct.2024.119113.

[17] X. Meng, L. Gardner, Hybrid construction featuring wire arc additive manufacturing: review, concepts, challenges and opportunities, Eng. Struct. 326 (2025) 119337, https://doi.org/10.1016/j.engstruct.2024.119337.

[18] P. Kyvelou, C. Huang, J. Li, L. Gardner, Residual stresses in steel I-sections strengthened by wire arc additive manufacturing, in: Structures 60, 2024, p. 105828, https://doi.org/10.1016/j.istruc.2023.105828.

[19] H. Dahaghin, M. Motavalli, H. Moshayedi, S.M. Zahrai, E. Ghafoori, Wire and arc additive manufacturing for strengthening of metallic components, Thin-Walled Struct. 203 (2024) 112074, https://doi.org/10.1016/j.tws.2024.112074.

[20] E. Ghafoori, H. Dahaghin, C. Diao, N. Pichler, L. Li, M. Mohri, J. Ding, S. Ganguly, S. Williams, Fatigue strengthening of damaged steel members using wire arc additive manufacturing, Eng. Struct. 284 (2023) 115911, https://doi.org/10.1016/j.engstruct.2023.115911.

[21] E. Ghafoori, H. Dahaghin, C. Diao, N. Pichler, L. Li, J. Ding, S. Ganguly, S. Williams, Metal 3D-printing for repair of steel structures, in: ce/papers 6, 2023, pp. 3–4, pp. 796–801, https://doi.org/10.1002/cepa.2285.

[22] J.G. Lopes, D. Martins, K. Zhang, B. Li, B. Wang, X. Wang, N. Schell, E. Ghafoori, A. C. Baptista, J.P. Oliveira, Unveiling the microstructure evolution and mechanical properties in a gas tungsten arc-welded Fe–Mn–Si–Cr–Ni shape memory alloy, J. Mater. Sci. (2024) 1–22, https://doi.org/10.1007/s10853-024-09606-4.

[23] I.O. Felice, J. Shen, A.F. Barragan, I.A. Moura, B. Li, B. Wang, H. Khodaverdi, M. Mohri, N. Schell, E. Ghafoori, T.G. Santos, J.P. Oliveira, Wire and arc additive manufacturing of Fe-based shape memory alloys: microstructure, mechanical and functional behavior, Mater. Des. 231 (2023) 112004, https://doi.org/10.1016/j.matdes.2023.112004.

[24] A. Jafarabadi, I. Ferretto, M. Mohri, C. Leinenbach, E. Ghafoori, 4D printing of recoverable buckling-induced architected iron-based shape memory alloys, Mater. Des. 233 (2023) 112216, https://doi.org/10.1016/j.matdes.2023.112216.

[25] M.H. Baqershahi, C. Ayas, E. Ghafoori, Design optimisation for hybrid metal additive manufacturing for sustainable construction, Eng. Struct. 301 (2024), https://doi.org/10.1016/j.engstruct.2023.117355, 117355.

[26] S. Kokare, J.P. Oliveira, T.G. Santos, R. Godina, Environmental and economic assessment of a steel wall fabricated by wire-based directed energy deposition, Additiv. Manufact. 61 (2023), https://doi.org/10.1016/j.addma.2022.103316. S. 103316.

[27] R.C. Reis, S. Kokare, J.P. Oliveira, J.C. Matias, R. Godina, Life cycle assessment of metal products: a comparison between wire arc additive manufacturing and CNC milling in: advances in industrial and manufacturing engineering, 6, S 100117, 2023, https://doi.org/10.1016/j.aime.2023.100117.

[28] S. Kokare, J.P. Oliveira, R. Godina, A LCA and LCC analysis of pure subtractive manufacturing, wire arc additive manufacturing, and selective laser melting approaches, J. Manuf. Process. 101 (2023) 67–85, https://doi.org/10.1016/j.jmapro.2023.05.102.

[29] A.C. Bekker, J.C. Verlinden, Life cycle assessment of wire + arc additive manufacturing compared to green sand casting and CNC milling in stainless steel, J. Clean. Prod. 177 (2018) 438–447, https://doi.org/10.1016/j.jclepro.2017.12.148.

[30] J. Liu, Y. Ma, Sustainable design-oriented level set topology optimization, J. Mech. Des. 139 (2017) H. 1, https://doi.org/10.1115/1.4035052.

[31] K. Hoschke, K. Kappe, S. Patil, S. Kilchert, J. Kim, A. Pfaff, Sustainability-oriented topology optimization towards a more holistic design for additive manufacturing, in: C. Klahn, M. Meboldt, J. Ferchow (Eds.), Industrializing Additive Manufacturing, Cham: Springer International Publishing, 2024, pp. 77–88.

[32] R.D. Kundu, X.S. Zhang, Sustainability-oriented multimaterial topology optimization: designing efficient structures incorporating environmental effects, Struct. Multidiscip. Optim. 68 (2025) H. 1, https://doi.org/10.1007/s00158-024-03930-8.

[33] L. Ryan, I.Y. Kim, A multiobjective topology optimization approach for cost and time minimization in additive manufacturing, Int. J. Numer. Methods Eng. 118, H. 7 (2019) 371–394, https://doi.org/10.1002/nme.6017.

[34] G. Sabiston, I.Y. Kim, 3D topology optimization for cost and time minimization in additive manufacturing, Struct. Multidiscip. Optim. 61, H. 2 (2020) 731–748, https://doi.org/10.1007/s00158-019-02392-7#Sec2.

[35] C. López, S. Burggraeve, P. Lietaert, J. Stroobants, X. Xie, S. Jonckheere, B. Pluymers, W. Desmet, Model-based, multi-material topology optimization taking into account cost and manufacturability, Struct. Multidiscip. Optim. 62, H. 6 (2020) 2951–2973, https://doi.org/10.1007/s00158-020-02641-0.

[36] I.H. Shah, N. Hadjipantelis, L. Walter, R.J. Myers, L. Gardner, Environmental life cycle assessment of wire arc additively manufactured steel structural components, J. Clean. Prod. 389 (2023) 136071, https://doi.org/10.1016/j.jclepro.2023.136071.

[37] P.C. Priarone, E. Pagone, F. Martina, A.R. Catalano, L. Settineri, Multi-criteria environmental and economic impact assessment of wire arc additive manufacturing, CIRP Ann. 69, H. 1 (2020) 37–40, https://doi.org/10.1016/j.cirp.2020.04.010.

[38] G. Campatelli, F. Montevecchi, G. Venturini, G. Ingarao, P.C. Priarone, Integrated WAAM-subtractive versus pure subtractive manufacturing approaches: an energy efficiency comparison, in: International Journal of Precision Engineering and Manufacturing-Green Technology 7, H. 1, S, 2020, pp. 1–11, https://doi.org/10.1007/s40684-019-00071-y.

[39] M. Dias, J.P.M. Pragana, B. Ferreira, I. Ribeiro, C.M.A. Silva, Economic and environmental potential of wire-arc additive manufacturing, Sustainability 14, Nr. 9 (2022) 5197, https://doi.org/10.3390/su14095197.

[40] S. Kokare, J. Shen, P.P. Fonseca, J.G. Lopes, C.M. Machado, T.G. Santos, J. P. Oliveira, R. Godina, Wire arc additive manufacturing of a high-strength low-alloy steel part: environmental impacts, costs, and mechanical properties, Int. J. Adv. Manuf. Technol. 134 (1–2) (2024) 453–475, https://doi.org/10.1007/s00170-024-14144-z.

[41] A.Z.A. Kadir, Y. Yusof, M.S. Wahab, Additive manufacturing cost estimation models—a classification review, Int. J. Adv. Manuf. Technol. 107 (9–10) (2020) 4033–4053, https://doi.org/10.1007/s00170-020-05262-5.

[42] F. Martina, S. Williams, Wire+arc additive manufacturing vs. traditional machining from solid: a cost comparison, 2015. https://waammat.com/documents/waam-vs-machining-from-solid-a-cost-comparison.

[43] C.R. Cunningham, S. Wikshåland, F. Xu, N. Kemakolam, A. Shokrani, V. Dhokia, S. T. Newman, Cost modelling and sensitivity analysis of wire and arc additive manufacturing, Procedia Manufac. 11 (2017) 650–657, https://doi.org/10.1016/j.promfg.2017.07.163.

[44] F. Facchini, A. Chirico, de; Mummolo, G., Comparative cost evaluation of material removal process and additive manufacturing in aerospace industry, in: International Joint Conference on Industrial Engineering and Operations Management, Springer, Cham, 2019, pp. 47–59.

[45] D. Fang, N. Brown, C. Wolf, de; Mueller, C., Reducing embodied carbon in structural systems: a review of early-stage design strategies 2352-7102 76 (2023) 107054, https://doi.org/10.1016/j.jobe.2023.107054.

[46] E. van de Ven, R. Maas, C. Ayas, M. Langelaar, F. van Keulen, Continuous front propagation-based overhang control for topology optimization with additive manufacturing, Struct. Multidiscip. Optim. 57 (2018) 2075–2091.

[47] E. van de Ven, R. Maas, C. Ayas, M. Langelaar, F. van Keulen, Overhang control based on front propagation in 3D topology optimization for additive manufacturing, Comput. Methods Appl. Mech. Eng. 369 (2020) 113169, https://doi.org/10.1016/j.cma.2020.113169.

[48] V. Mishra, C. Ayas, M. Langelaar, F. van Keulen, A stress-based criterion to identify and control intersections in 2D compliance minimization topology optimization, Struct. Multidiscip. Optim. 65, H. 11 (2022) 1–19, https://doi.org/10.1007/s00158-022-03424-5.

[49] M.P. Bendsøe, Optimal shape design as a material distribution problem, Struct. Multidiscip. Optim. 1, H. 4 (1989) 193–202, https://doi.org/10.1007/BF01650949.

[50] O. Sigmund, J. Petersson, Numerical instabilities in topology optimization: a survey on procedures dealing with checkerboards, mesh-dependencies and local minima, Struct. Multidiscip. Optim. 16, H. 1 (1998) 68–75, https://doi.org/10.1007/BF01214002.

[51] T.E. Bruns, D.A. Tortorelli, Topology optimization of non-linear elastic structures and compliant mechanisms, Comput. Methods Appl. Mech. Eng. 190 (26–27) (2001) 3443–3459, https://doi.org/10.1016/S0045-7825(00)00278-4.

[52] F. Wang, B.S. Lazarov, O. Sigmund, On projection methods, convergence and robust formulations in topology optimization, Struct. Multidiscip. Optim. 43, H. 6 (2011) 767–784, https://doi.org/10.1007/s00158-010-0602-y.

[53] F. Ferrari, O. Sigmund, A new generation 99 line Matlab code for compliance topology optimization and its extension to 3D, Struct. Multidiscip. Optim. 62, H. 4 (2020) 2211–2228, https://doi.org/10.1007/s00158-020-02629-w.

[54] K. Svanberg, The method of moving asymptotes—a new method for structural optimization, Int. J. Numer. Methods Eng. 24, Nr. 2 (1987) 359–373, https://doi.org/10.1002/nme.1620240207.

[55] M.A.J. Huijbregts, Z.J.N. Steinmann, P.M.F. Elshout, G. Stam, F. Verones, M. Vieira, M. Zijp, A. Hollander, R. van Zelm, ReCiPe2016: a harmonised life cycle impact assessment method at midpoint and endpoint level, Int. J. Life Cycle Assess 2 (2017) 138–147, https://doi.org/10.1007/s11367-016-1246-y.